BorneoScience
The Journal of Science & Technology
Volume 43 Issue 2 : Oct 2022
Online ISSN : 2231-9085 | ISSN : 1394-4339

ADSORPTION OF 2,4-DICHLOROPHENOL (2,4-DCP) ONTO ACTIVATED CARBON DERIVED FROM COFFEE WASTE

S M Anisuzzaman[1], Collin G. Joseph[2,*], Mintshe Tan[2]

[1]Chemical Engineering Programme, Faculty of Engineering,
Universiti Malaysia Sabah, 88400 Kota Kinabalu, Sabah, Malaysia.
[2]Industrial Chemistry Programme, Faculty of Science and Natural Resources,
Universiti Malaysia Sabah, 88400 Kota Kinabalu, Sabah, Malaysia.

[*]Corresponding author: collin@ums.edu.my

Received 23th June 2021; accepted 11th July 2022
Available online 1st Nov 2022

ABSTRACT. *In this study, activated carbons (ACs) were prepared from coffee waste via a two-stage self-generated atmosphere method after impregnation by zinc chloride ($ZnCl_2$). The effect of impregnation ratio (IR) on the physicochemical properties and adsorption capacity for 2,4-dichlorophenol (2,4-DCP) was studied. Characterizations of the generated ACs were carried out to determine the percentage of yield, moisture and ash contents, pH, surface chemistry studies and morphological attributes. The results showed that the yield of AC decreased from 41.16% to 37.12% with the increase in IR. As for moisture and ash contents, the percentage values ranged from 4.18% to 6.16% and 9.73% to 10.34% respectively. Meanwhile, the AC samples were slightly acidic with pH values varying between 6.06 and 6.56. The adsorption capacity increased from 16.8 mg/g for AC1 to 21.72 mg/g for AC4. The AC produced with an IR of 4:1 (AC4) had the highest adsorption capacity of 2,4-DCP, which was 21.72 mg/g. The maximum Brunauer, Emmett and Teller (BET) surface area of the best produced AC4 was found to be 951.10 m^2/g, which is by far the highest achieved in comparison with other coffee waste-derived ACs reported in the literature. N_2 adsorption-desorption graph showed a Type I isotherm, indicating that the AC4 was a microporous solid with chemisorption properties. Langmuir isotherm model was found to be a better fit for the adsorption data when compared to the Freundlich isotherm model. Pseudo-second order kinetic model was best described for the kinetic of 2,4-DCP adsorption. This proved that 2,4-DCP adsorption by AC4 was a chemisorption process.*

KEYWORDS: Activated carbon, two-stage activation, 2,4-dichlorophenol, coffee waste, adsorption

INTRODUCTION

Chlorophenols are one of the pollutants of emerging concern commonly found in polluted water. This is because chlorophenols are widely used in chemical industries as pesticides, petroleum

refineries process, wood preservation, and bleaching process in the pulp and paper industry. Chlorophenols have been categorized as hazardous materials since they are carcinogenic, mutagenic, and teratogenic. Moreover, phenolic compounds (PCs) properties may contribute to rapid absorption through contact with nasal, oral, eye or skin and dermal contact. Chlorophenols can permeate through human skin and a sufficient dose of chlorophenols can cause liver damage, chronic bronchitis, cough, and even death [1,2]. The removal of chlorophenols from the environment is crucial because of their structural stability and persistence in the environment and to prevent the exposure of chlorophenols to living organisms [3-5]. Due to their toxicity, phenols have been included in the Malaysian government's list of priority contaminants. According to National Water Quality Standards for Malaysia, the phenol compounds should be less than 10 mg/l in water surface. Consequently, the removal or biodegradation/bioconversion of PC from wastewater is necessary before it is released into water bodies. Numerous research studies have been conducted to develop sustainable technology in the PCs contaminated industrial effluents [6-9].

Adsorption technology has gained some attention in PCs containing wastewater treatment processes since it is versatile in design, simple operation, and effective regeneration of adsorbents via desorption [10-12]. Moreover, this technology is also able to extract PC at low concentrations [13]. However, the quality of the adsorption mechanism was highly reliant on the adsorbent material used in the process. In wastewater treatment, the removal of various pollutants using activated carbon (AC) has been proven to be faster than other chemical and physical methods, such as biological treatment, photochemical treatment, and electrochemical oxidation [14-16]. AC is a highly porous material with an amphoteric character on its surface. Besides that, AC has high mechanical strength, thermo-stability, adequate pore size distribution, and low acid/base reactivity [17-20]. However, commercial AC is produced from expensive precursor materials; its usage has been narrowed. Hence, cheaper precursor materials such as agricultural waste have been utilised to produce AC [21-22].

One precursor material that has been used to generate AC in many studies is coffee waste [23-29]. Coffee waste is the solid residue of the coffee bean after the flavour had been extracted to make coffee beverages. Coffee waste is utilised as precursor material because a great quantity of coffee waste is produced annually since coffee is one of the essential agricultural commodities in the world. Besides that, recycling the coffee waste to produce AC is environmentally friendly due to coffee waste needing large amounts of oxygen for degradation. Furthermore, coffee provides a waste-to-wealth opportunity in which a low-cost AC can be produced from it. Its low ash content and high availability make it an ideal precursor for producing AC [27-29].

Therefore, in this study, coffee waste as precursor material was used to prepare the AC with different impregnation ratios (IR) of zinc chloride ($ZnCl_2$) to precursor using two-stage chemical activation under a self-generated atmosphere for the removal of 2,4-Dichlorophenol (2,4-DCP) in the aqueous medium. The initial concentration of chlorophenols, adsorbent dosage, and solution pH were varied in batch adsorption test to study the adsorption of chlorophenols by AC. The AC was characterised by utilizing moisture and ash content test, Fourier-transform infrared (FT-IR) spectroscopy, and scanning electron microscopy (SEM).

MATERIALS AND METHODOLOGY

Chemicals and instruments

The chemicals utilised in this study were zinc chloride ($ZnCl_2$) from EMSURE®, methanol (CH_3OH) from Fisher Scientific UK, 2,4-dichlorophenol (2,4-DCP), hydrochloric acid (HCl), and sodium hydroxide (NaOH) from Sigma-Aldrich. All chemicals were used without further purification. The instruments used in this study were FT-IR spectrometer (Thermo Nicolet Nexus 670 FTIR, Thermo Scientific), muffle furnace (CWF 1200, CARBOLITE), scanning electron microscope (SEM) (JSM-5610 LV, JEOL), and Ultraviolet–visible (UV-Vis) spectrophotometer (Agilent Cary 60 UV-Vis, Agilent Technologies).

Preparation of coffee waste

Coffee waste was employed as the precursor material for the preparation of AC and was obtained from the local restaurants in Kota Kinabalu, Sabah, Malaysia. The coffee waste was washed with hot water to remove dust, impurities, and water-soluble substances. Then, it was rewashed with distilled water and dried in an oven for 24 h at 110°C to reduce the moisture content of coffee waste [29]. The dried coffee waste was stored in a desiccator to prevent moisture uptake.

Preparation of AC

A two-stage self-generated atmosphere method was used to prepare the AC from dried coffee waste. The precursor was semi-carbonized (first stage), and then subjected to an activation process (second stage) after impregnating the semi-carbonised char with $ZnCl_2$. $ZnCl_2$ was used for the impregnation process as the prepared AC will have a great surface area, and more micropores but lesser mesopores [30]. Both semi-carbonization and activation were done in a self-generated atmosphere. Self-generated atmosphere is the atmosphere that consists of the volatile matter which is generated from the pyrolysis process. The dried coffee waste was divided into 5 batches and labelled as AC1, AC2, AC3, AC4, and AC5 respectively. These samples were weighed using an electronic balance and the weight of each sample was recorded as W_o (g). Then, these samples were put into the muffle furnace and semi-carbonised at 300°C for 1 h under self-generated atmosphere[31]. After the semi-carbonisation process, the samples were left in the muffle furnace to cool down to room temperature and kept in a desiccator.

Activation process

The AC1 was agitated with the $ZnCl_2$ solution at an IR of 1:1 at 85°C using a hot plate and stirred with a magnetic bar until the solution in the beaker was completely dried. After that, AC1 was activated in the muffle furnace at 500°C for 2 h under a self-generated atmosphere and left to cool down to room temperature [31]. The resulted AC1 was boiled with 0.01M hydrochloric acid (HCl) for 1 h and washed thoroughly with hot distilled water to remove the residual $ZnCl_2$ until the washing solution reached pH 6 – 7. Finally, AC1 was dried in the oven at 110°C for 24 h. The dried AC1 was weighed, and its weight was recorded as W_{DAC}(g). These procedures were repeated for AC2 – AC5 of which the $ZnCl_2$ was added in the ratio of 2:1, 3:1, 4:1, and 5:1 respectively. Table 1 showed the semi-carbonisation and activation conditions of AC1 – AC5.

Table 1. Semi-carbonisation and activation conditions of AC1 – AC5

Samples	Semi-carbonisation		Activation		
	Time (h)	Temperature (°C)	IR ($ZnCl_2$:AC)	Time (h)	Temperature (°C)
AC1	1	300	1:1	2	500
AC2	1	300	2:1	2	500
AC3	1	300	3:1	2	500
AC4	1	300	4:1	2	500
AC5	1	300	5:1	2	500

Determination of percentage of yield

The percentage of yield was calculated based on the equation 1.

$$Percentage\ of\ yield\ (\%) = \frac{W_f}{W_i} x\ 100\% \quad (1)$$

where, W_f is the initial mass of the dry impregnated sample; W_i is the he final mass of the sample after activation process is complete

Determination of moisture and ash contents

In order to determine the moisture content, 1 g of AC1 was weighed in a tarred petri dish with cover. Then, AC1 in the tarred petri dish was dried in the oven at 145 - 155°C for 3 h with the cover removed. The sample was covered and left to cool to room temperature. The cooled AC1 was weighed immediately. These steps were repeated for AC2 – AC5. The moisture content was calculated through equation 2.

$$Moisture\ content\ (\%) = \frac{Initial\ weight\ (g) - Final\ weight\ (g)}{Initial\ weight\ (g)} x\ 100\% \quad (2)$$

In the determination of ash content, the crucible was heated in a muffle furnace for 1 hour at 650 $\pm$ 25°C and weighed after it was cooled. The dried AC1 from the moisture content test was put into the crucible and weighed before heating in a muffle furnace at 650 $\pm$ 25°C from 3 - 16 h until the carbon was completely burnt. The sample was left to cool to room temperature and weighed immediately. These steps were repeated for AC2 – AC5. The ash content was calculated by equation 3.

$$Ash\ content\ (\%) = \frac{Weight\ of\ the\ sample\ after\ ash\ process}{Weight\ of\ the\ sample\ before\ ash\ process}\ x\ 100\% \quad (3)$$

Determination of pH

1 g of dried AC1 was put into a 250 ml Erlenmeyer flask and 100 ml of hot distilled water was poured into the same flask. The mixture was boiled gently for 15 minutes and the AC1 in the mixture was filtered out using vacuum filtration. The filtrate was collected and cooled to 50 $\pm$ 5°C. The pH of the filtrate was measured using the pH meter. These procedures were repeated for AC2 – AC5.

Surface chemistry studies

The surface chemistry was studied using FT-IR spectroscopy. A small amount of coffee waste, AC samples, and KBr powder were firstly dried in oven at 110°C for 24 h. Then, the coffee waste and AC samples were crushed into powder form and mixed with KBr respectively. After that, the mixture was made into a transparent disc and tested with a FT-IR spectrometer. The FT-IR spectroscopy was carried out under room temperature in the wavenumber range from 4000 cm^{-1} to 400 cm^{-1} with 2 cm^{-1} resolution.

Morphological studies

The morphology of coffee waste and AC were investigated utilising SEM method. The AC samples were sieved to get the granular form. After that, a small amount of coffee waste and granular AC samples were dried for 24 h at 110°C in an oven before analyse using SEM.

Chlorophenols adsorption experiment

The adsorption equilibrium and adsorption kinetics studies were performed using batch adsorption method. The effects of initial concentration, adsorbent dosage, and solution pH on the 2,4-DCP adsorption of AC with the highest adsorption capacity of 2,4-DCP were studied.

Preparation of 2,4-DCP Solution

The λ_{max} of 2,4-DCP is 280nm. In order to prepare 1000 mg/l of the 2,4-DCP solution, 1 g of 2,4-DCP powder was weighed and dissolved using 10 ml of methanol in a beaker. Then, the solution was diluted in a 1000 ml volumetric flask. A magnetic bar was put into the volumetric flask and the solution was stirred on a hot plate for 1 hour. After that, the desired concentration of the 2,4-DCP solution was prepared from the 1000 mg/l of 2,4-DCP solution through the dilution method.

Adsorption capacity test

The AC samples (AC1 – AC5) were sieved to get the granular form AC. 0.5 g of granular AC samples and 600 ml of 20 mg/l 2,4-DCP solution were put into a beaker. The mixture was stirred using a hot plate and magnetic bar for 3 hours at room temperature. The AC samples were filtered out and the 2,4-DCP uptake at equilibrium was analysed using the UV-Vis spectrophotometer. The objective of this test was to find an AC sample with the largest adsorption capacity of 2,4-DCP for the following procedures. The 2,4-DCP uptake at equilibrium was calculated by equation 4.

$$Q_e = \frac{(C_i - C_e)V}{W} \quad (4)$$

where, Q_e (mg/g) is the 2,4-DCP uptake at equilibrium, C_i and C_e (mg/l) are the liquid-phase concentration of 2,4-DCP at initial and equilibrium respectively, V(l) is the volume of the solution, and W (g) is the mass of AC used.

Effect of initial concentration

In order to study the effect of initial concentration on the 2,4-DCP adsorption, different concentrations (5, 10, 15, and 20 mg/l) of 2,4-DCP solution were prepared in volumetric flasks. 600 ml of each of the 2,4-DCP solutions was poured into 4 beakers respectively. Next, 0.5 g AC was added into the beakers separately. The beakers were placed on a hot plate and stirred using a magnetic

bar for 3 h and then the AC was filtered out. The 2,4-DCP uptake at equilibrium was analysed using the UV-Vis spectrophotometer and calculated using equation 4.

Effect of Adsorbent Dosage

0.1, 0.3, and 0.5 g of AC were added respectively into 3 beakers which contained 600 ml of 2,4-DCP solution with a concentration of 20 mg/l . The mixture was stirred for 3 h and the 2,4-DCP adsorption capacity was analysed using the UV-Vis spectrophotometer and calculated using equation 4. In addition, the percentage of removal was determined from equation 5.

$$Percentage\ of\ removal\ (\%) = \frac{(C_i - C_e)}{C_i} x100\% \quad (5)$$

Effect of Solution pH

600 ml of 20 mg/l 2,4-DCP solution was poured into an Erlenmeyer flask. The pH of the 2,4-DCP solution was altered to 3, 7, and 9 by adding HCl and NaOH solutions with different concentrations (0.01 M and 0.1 M). After that, 0.5 g of AC samples were added into the Erlenmeyer flasks that contain 2,4-DCP solution with different pH respectively. The mixture was stirred for 3 h using a hot plate and magnetic bar. Then, the sample solutions were filtered using 0.45 µm polytetrafluoroethylene (PTFE) syringe filter and put into a quartz cuvette. The residual concentration of 2,4-DCP was determined through a UV-Vis spectrophotometer.

Adsorption kinetics studies

600 ml of 20 mg/l 2,4-DCP solution and 0.5 g of AC sample were added into a beaker. The mixture was agitated utilising a hot plate and a magnetic bar for 200 min. The aqueous samples were taken at every 10 min for UV-Vis spectrophotometer analysis [43]. The 2,4-DCP uptake at time t, Q_t (mg/g) was calculated by equation 6.

$$Q_t = \frac{(C_i - C_t)V}{W} \quad (6)$$

where C_i is the initial adsorbate concentration at given time (mg/l); C_t is the equilibrium adsorbate concentration at given time (mg/l); V (l) is the volume of the solution, and W (g) is the mass of AC used.

The adsorption kinetics of AC on chlorophenols was evaluated through pseudo-first-order, pseudo-second-order and intraparticle diffusion models. The equations of pseudo-first order, pseudo-second order and intraparticle diffusion models are as bellows respectively.

$$ln\ ln\ (Q_e - Q_t) = -K_1 t + ln\ ln\ Q_e \quad (7)$$

where, Q_t is the amount of adsorbate adsorption at time (mg/g); K_1 is the Pseudo-first order adsorption rate constant (hr^{-1}); t the is mixing time (hr); Q_e is the amount of adsorbate adsorption at equilibrium (mg/g)

$$\frac{t}{Q_t} = \frac{t}{Q_e} + \frac{1}{K_2 Q_e^2} \quad (8)$$

where, Q_t is the amount of adsorbate adsorption at time (mg/g); K_2 is the Pseudo-second order adsorption rate constant (g/mg.hr); t is the Mixing time (hr); Q_e is the amount of adsorbate adsorption at equilibrium (mg/g)

$$Q_t = k_{id} t^{1/2} + a \quad (9)$$

where k_{id} (mg/g min$^{1/2}$) is the intraparticle diffusion rate constant, a (mg/g) is a constant in the intraparticle diffusion model, which reflects the significance of the boundary layer or mass transfer effect.

Adsorption isotherms studies

The equilibrium data was fitted to the Langmuir and Freundlich isotherm models to show the most suitable correlation for the adsorption system. The equations of Langmuir and Freundlich isotherm models are listed in equations 10 and 11 correspondingly.

$$\frac{C_e}{Q_e} = \frac{C_e}{Q_{max}} + \frac{1}{K_L Q_{max}} \quad (10)$$

where, Q_{max} is the maximum monolayer adsorption capacity (mg/g); K_L is the Langmuir isotherm constant (mg/l); C_e is the Equilibrium adsorbate concentration (mg/l); Q_e is the amount of adsorbate adsorption at equilibrium (mg/g)

$$In\ Q_e = In\ K_f + \frac{1}{n} In\ C_e \quad (11)$$

where, Q_e is the adsorption density at the equilibrium solute concentration (mg adsorbate/g adsorbent); C_e is the equilibrium concentration of adsorbate in solution (mg/l); K_f is the Freundlich adsorption capacity constant (mg/g); n is the adsorption intensity (mg/g)

RESULTS AND DISCUSSION

The physical appearance of washed and dried coffee waste was slightly different from the raw coffee waste. The surface of washed and dried coffee waste was less shiny and had shrunk slightly due to the loss of moisture content from the coffee waste. After the semi-carbonisation and activation processes, the brownish-black coffee waste had changed into fragile black AC. Furthermore, the AC had lost its original coffee fragrance. The prepared AC samples (AC1 – AC5) were characterised via the percentage of yield, moisture and ash contents, pH, surface chemistry and morphological studies.

Physical characterization

The yield, moisture and ash content percentage along with pH of AC1-AC5 are shown in Table 2.

Table 2. Percentage of yield, moisture and ash contents, and pH of AC1 – AC5

Samples	Yield (%)	Moisture content (%)	Ash content (%)	pH
AC1	41.16	4.56	9.73	6.18

AC2	40.61	4.18	9.88	6.06
AC3	38.16	5.22	9.96	6.36
AC4	37.35	6.16	10.17	6.56
AC5	37.12	5.01	10.34	6.54

Based on Table 2, the results showed that the yield of AC decreased from 41.16% to 37.12% with the increase in IR. The decrease in yield was due to the formation of mesopore in AC which is induced by the $ZnCl_2$. As the IR increased to above 1:1, the initial function of $ZnCl_2$ during activation which is the inhibition of volatile matter would be lost. During activation, the volatile matters will be discharged from the carbon surface since their movement through the pore passages will not be inhibited [32]. Consequently, the pores will start to widen and collapse due to the increased pyrolytic decomposition as IR is further increased [46]. This in turn leads to the weight loss in the precursor at the activation stage.

As can be seen from Table 2, the moisture contents of five AC samples were ranged from 4.18% to 6.16%. AC2 had the lowest moisture content, 4.18% whereas AC4 had the highest moisture content, 6.16%. In comparison, the moisture contents of AC1 – AC5 were slightly lower than in the previous study carried out by Boonamnuayvitaya *et. al.* [28] in which the moisture contents ranged from 5.36% to 12.63%. The moisture in AC was due to the uptake of moisture in the atmosphere. This result indicated that IR does not influence the moisture content of AC.

From the outcome obtained, it was proven that the ash content of AC was increased with the increasing IR. This is because more inorganic compounds are formed and more carbon atoms are consumed as IR is increased. AC1 recorded the lowest ash content, 9.73% and AC5 recorded the highest ash content, 10.34%. On the other hand, the ash contents of AC1 – AC5 was higher than other ACs that were prepared from different precursors. For instance, the ash content of AC prepared from the grape stalk in 1:1 IR was 1.16%.

The prepared AC samples (AC1 – AC5) were found to be slightly acidic as seen in Table 2. AC2 had the lowest pH value which was 6.06, whereas AC4 had the highest pH value which was 6.56. The acidic character of AC samples indicated that their surface contains more oxygen-containing groups (carboxylic, anhydrides, lactones, and phenols) than oxygen-free Lewis sites, carbonyls, pyrone, and chromene-type structures. Besides that, the acidic wash utilised HCl also contributed to this outcome. The pH values obtained were found to be compatible with the research of Namanea *et. al.* [29] in which their AC made from the coffee ground by $ZnCl_2$ activation had pH of 6.36.

Surface chemistry studies of AC

The FT-IR spectra of coffee waste and AC1 – AC5 are shown in Figure 1. The FT-IR spectrum of coffee waste showed a broad band at 3443.76 cm^{-1} which was attributed to -OH stretching vibration from carboxyls, phenols or alcohols. The band at 2927.56 cm^{-1} was corresponded to C-H stretching vibration and generally indicated the presence of an alkane group. Moreover, the peak at 2353.62 cm^{-1} indicated the C≡C stretching and the peak at 1645.98 cm^{-1} indicated the C=C stretching vibration from alkenes or C=O stretching vibration from aldehydes, ketones, carboxylic acids or esters. The band at 1383.44 cm^{-1} was resulted from C-H bending of methyl group or C-N stretching from amines

or amides. Furthermore, the C-O stretching from alcohols, ethers, carboxylic acids or esters produced a peak at 1067.49 cm^{-1} and the peak at 671.45 cm^{-1} was assigned to C-H out-of-plane bending in benzene derivatives or C-Cl stretching vibration.

On the other hand, the FT-IR spectra of AC1 – AC5 generally demonstrated a similar pattern. The broad band at 3452 cm^{-1} – 3417 cm^{-1} indicated the –OH stretching vibration, the band at 2367 cm^{-1} – 2349 cm^{-1} was attributed to C≡C stretching vibration and the band at 1628 cm^{-1} – 1614 cm^{-1} was assigned to C=C stretching vibration. Furthermore, the peak at 1387 cm^{-1} – 1383 cm^{-1} was attributed to C-H bending, the peak at 1103 cm^{-1} – 1089 cm^{-1} indicated the C-O stretching vibration, and the peak at 675 cm^{-1} – 671 cm^{-1} was assigned to C-H out-of-plane bending.

As compared with the FT-IR spectrum of coffee waste, there were missing peaks observed in the spectra of AC1 – AC5. The most significant observation was the disappearance of the peak at 2927.56 cm^{-1} as shown in Figure 1. This may be due to the decomposition of cellulose, hemicelluloses, and lignin, as well as the elimination of hydrogen in the coffee waste after activation process [33,34].

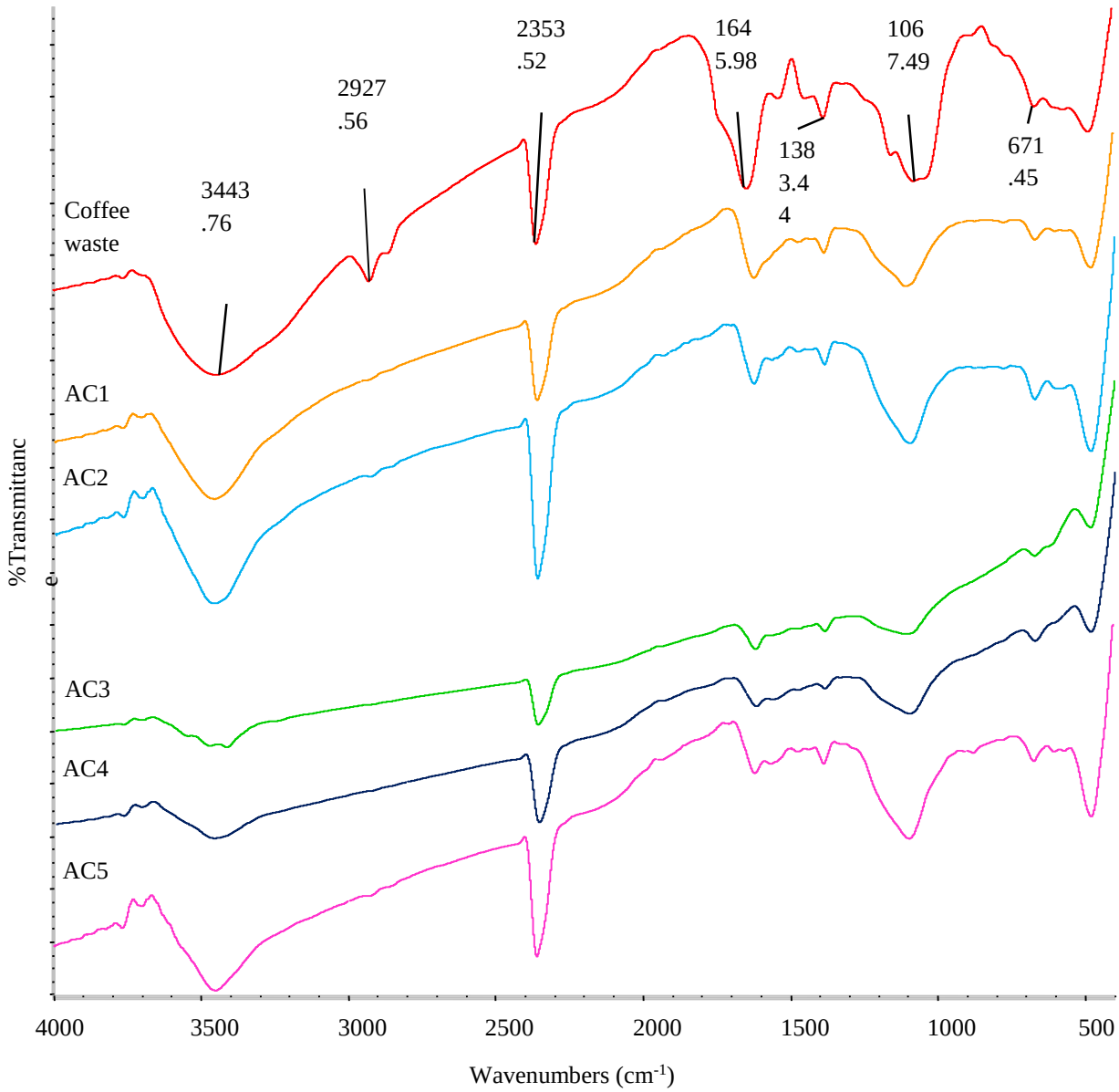

Figure 1. FT-IR spectra of coffee waste and AC1 – AC5.

Table 3 summarizes the peak identification of FTIR spectra on coffee waste and AC1 – AC5 samples.

Table 3. Peak Identification of FTIR spectra on coffee waste and AC1 – AC5

Sample	Band position (cm^{-1})	Possible Functional Group
Coffee waste	3443.76	-OH stretching
	2927.56	C-H stretching
	2353.62	C≡C stretching
	1645.98	C=C stretching
	1383.44	C-H bending
	1067.49	C-O stretching
	671.45	C-H out-of-plane bending
AC1 – AC5	3452 – 3417	-OH stretching
	2927.56	Undetected
	2367 – 2349	C≡C stretching
	1628– 1614	C=C stretching
	1387 cm^{-1} – 1383	C-H bending
	1103 cm^{-1} – 1089	C-O stretching
	675 cm^{-1} – 671	C-H out-of-plane bending

Morphological studies of AC

Scanning electron microscopy (SEM) was used to study the morphological structure of the prepared AC (Figure 2). The observation proved that different IR of $ZnCl_2$ can give different surface morphology to the produced AC. The surface structure of AC1 and AC2 comprised of cavities and pores of different shapes and sizes as shown in Figure 2 (b) and Figure 2 (c). Meanwhile, AC3 appeared to have a honeycomb-like structure as illustrated in Figure 2 (d). The morphology of AC4 which was observed from Figure 2 (e) showed that it had many cracks and irregular pores. Furthermore, irregular pores also existed for the morphology of AC5 as seen from Figure 2 (f). These pore structures are formed from the evaporation of $ZnCl_2$ and volatile matters during the activation process, leaving behind the voids which is formerly occupied by them [30,35].

In comparison, the rough and highly folded surface of coffee waste (Figure 2 a) was changed to AC1 – AC5 with a porous surface (Figure 2 (b-f)) after activation by $ZnCl_2$. This further verifies that $ZnCl_2$ is an activating agent. Besides that, the morphology of AC1 and AC2 showed smoother surfaces and had fewer voids than other AC samples. Although AC4 did not have a regular pore structure like AC3, it had more crevices and smaller pores compared to AC3. Meanwhile, AC5 had larger and crooked pores with the absence of small pores compared to AC4. Additionally, from the micrograph, it is evident that the pores of AC5 were starting to collapse compared to others AC samples. These indicate that increasing IR would generate AC with more pores but eventually, the pores would collapse because of the intense chemical attack by $ZnCl_2$.

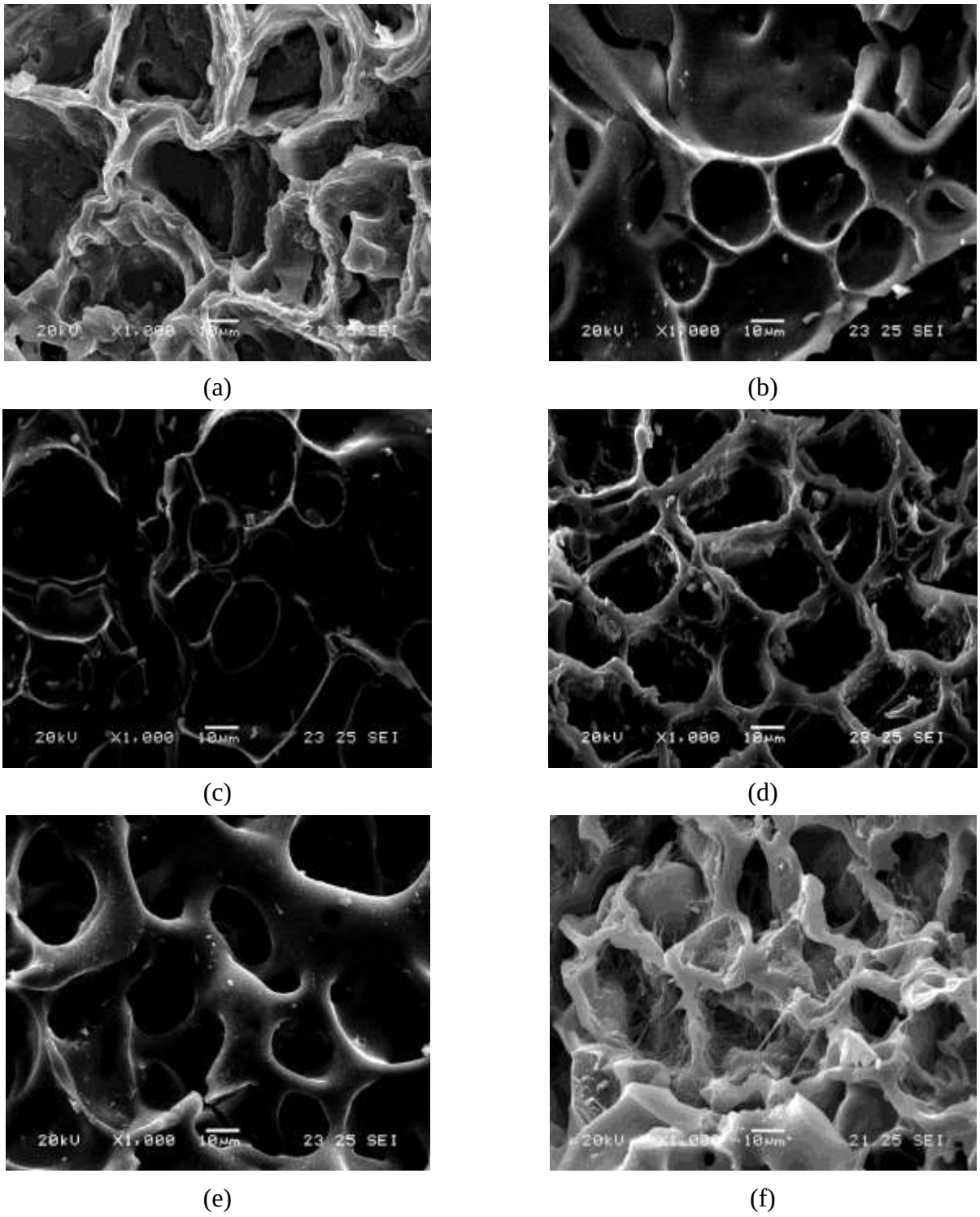

Figure 2. SEM micrographs (x1000 magnification) of (a) coffee waste (b) AC1 (c) AC2 (d) AC3 (e) AC4 (f) AC5

Specific surface area and pore-distribution

AC4 was selected for surface area and pore distribution analysis. The maximum Langmuir surface area of 951.10 m^2/g and the average pore diameter of 23.25 Å are comparable with other researchers' findings [36,37]. Table 4 represents the porous and surface characteristics of AC3.

Table 4. Surface area, pore volume and pore size of AC4

Surface area	
Langmuir surface area, m^2/g	$9.511x10^2$
BJH method cumulative adsorption surface area, m^2/g	$1.329x10^3$
BJH method cumulative desorption surface area, m^2/g	$1.325x10^3$
Pore volume	
BJH method cumulative adsorption pore volume, cc/g	0.4748
BJH method cumulative desorption pore volume, cc/g	0.4685
Pore size	
Average pore diameter, Å	23.25
BJH method adsorption pore diameter (mode), Å	8.870
BJH method desorption pore diameter (mode), Å	9.164

Figure 3 shows N_2 adsorption isotherm for coffee waste. N_2 adsorption-desorption graph showed a Type I isotherm, indicating that the AC4 was a microporous solid with chemisorption properties.

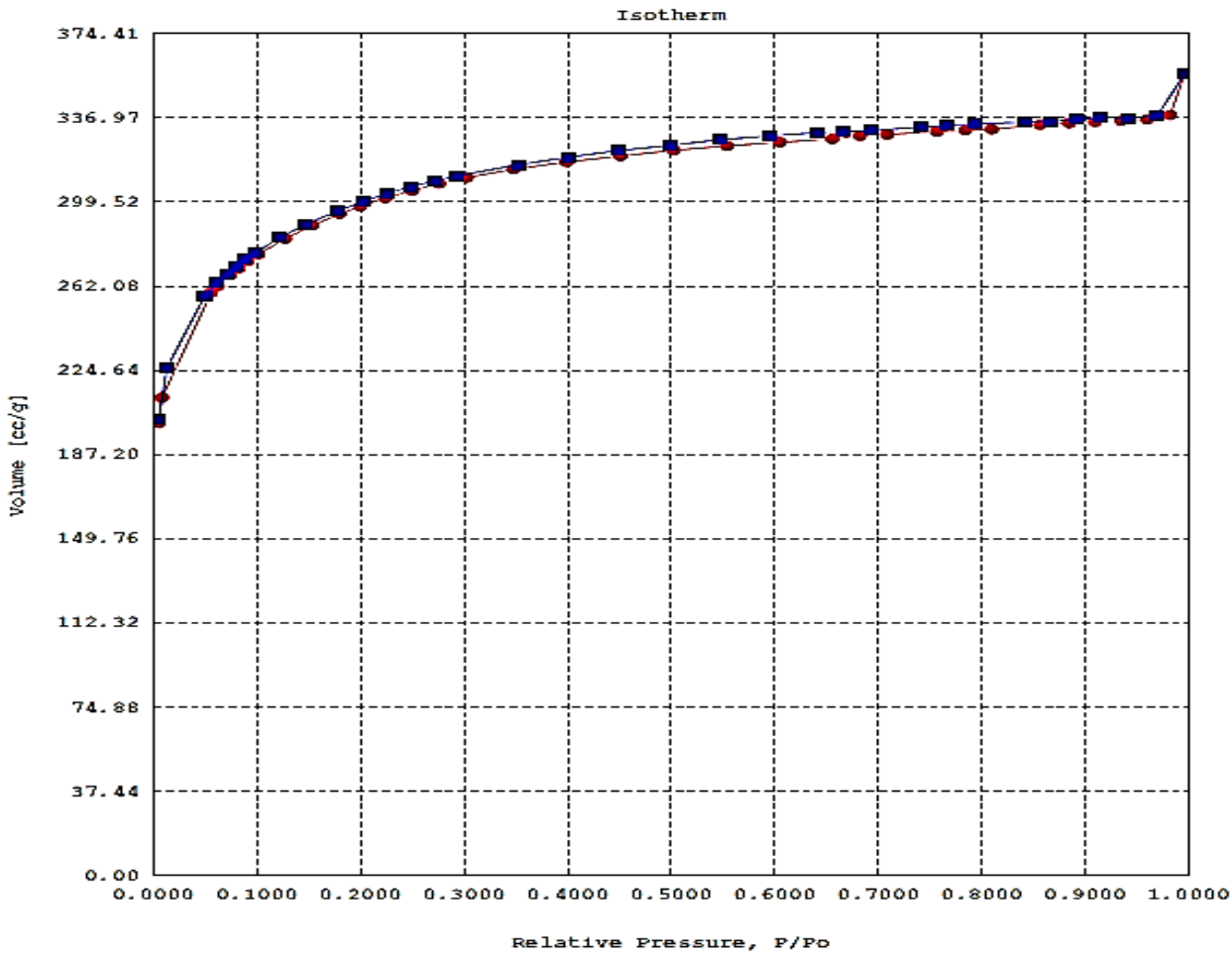

Figure 3. N_2 adsorption isotherm for coffee waste

Adsorption capacity test

The 2,4-DCP adsorption capacity test indicated that an increase in the IR would increase the adsorption capacity of AC. The adsorption capacity increased from 16.8 mg/g for AC1 to 21.72 mg/g for AC4. This is due to the development of micropore and mesopore of AC which increased proportionally with the IR. In consequence, the larger the number of pores, the higher the 2,4-DCP adsorption capacity of AC. This result proved that AC4 had the highest adsorption capacity which was compatible with the SEM micrograph of AC4 (Figure 2e) that illustrated a large number of pores. However, the adsorption capacity for AC5 dropped to 20.40 mg/g, indicating that further increases in the IR will destroy the pores of AC and hence decrease the adsorption capacity. The AC4 was utilised in the following 2,4-DCP adsorption tests. Table 5 shows the adsorption capacity of AC1 – AC5.

Table 5. Adsorption capacity of AC1 – AC5.

Samples	Adsorption capacity (mg/g)
AC1	16.80
AC2	18.72
AC3	19.32
AC4	21.72
AC5	20.40

Effect of initial concentration

In the effect of initial concentration, the amount of 2,4-DCP adsorbed by AC4 increased as the initial concentration was increased as shown in Figure 4. When the initial concentration was increased from 5 mg/l to 20 mg/l , the amount of 2,4-DCP adsorbed increased from 5.76 mg/g to 21.6 mg/g. This is because more 2,4-DCP available for AC to adsorb and the higher initial concentration provides a greater driving force for the mass transfer between 2,4-DCP and AC. Therefore, the adsorption efficiency of AC4 also increased.

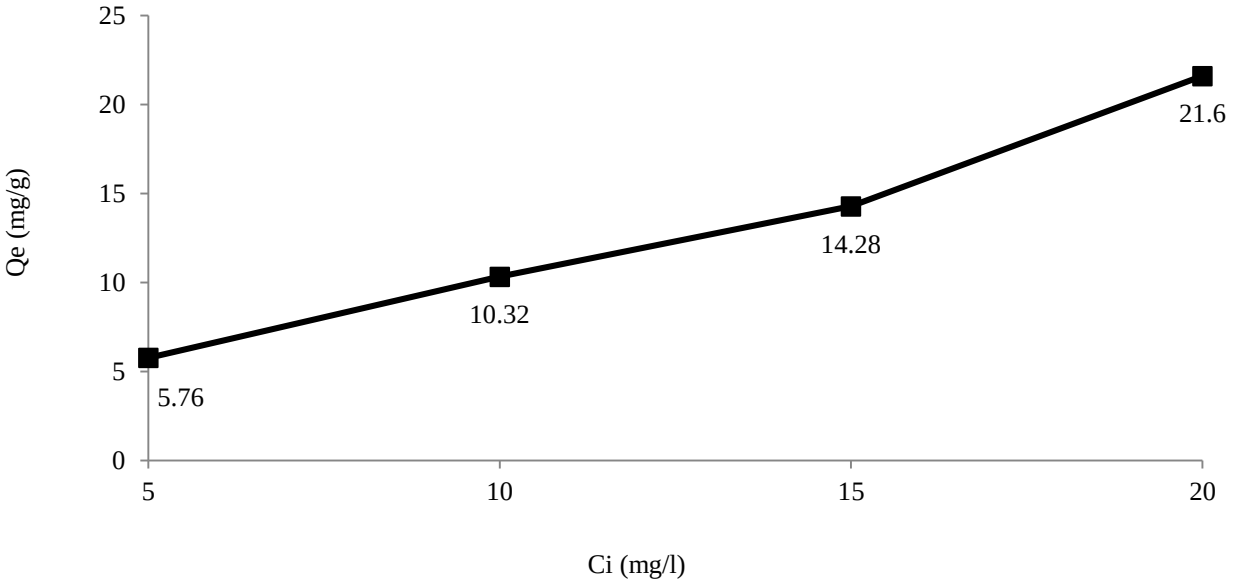

Figure 4. Amount of 2,4-DCP adsorbed, Q_e against initial concentration of 2,4-DCP

Effect of adsorbent dosage

The effect of adsorbent dosage on the removal of 2,4-DCP is presented in Figures 5 and 6. The amount of 2,4-DCP uptake decreased from 43.80 mg/g to 20.76 mg/g as the adsorbent dosage increased. This trend is due to the unsaturation of adsorption sites caused by the low concentration of adsorbate. There is also a that the large quantity of AC present would agglomerate and eventually cause decrement in the total surface area of AC. However, the removal percentage increased from 36.5% to 86.5% along with the increased adsorbent dosage. This is because more adsorption sites are available for the adsorption of 2,4-DCP and hence more 2,4-DCP molecules can be removed.

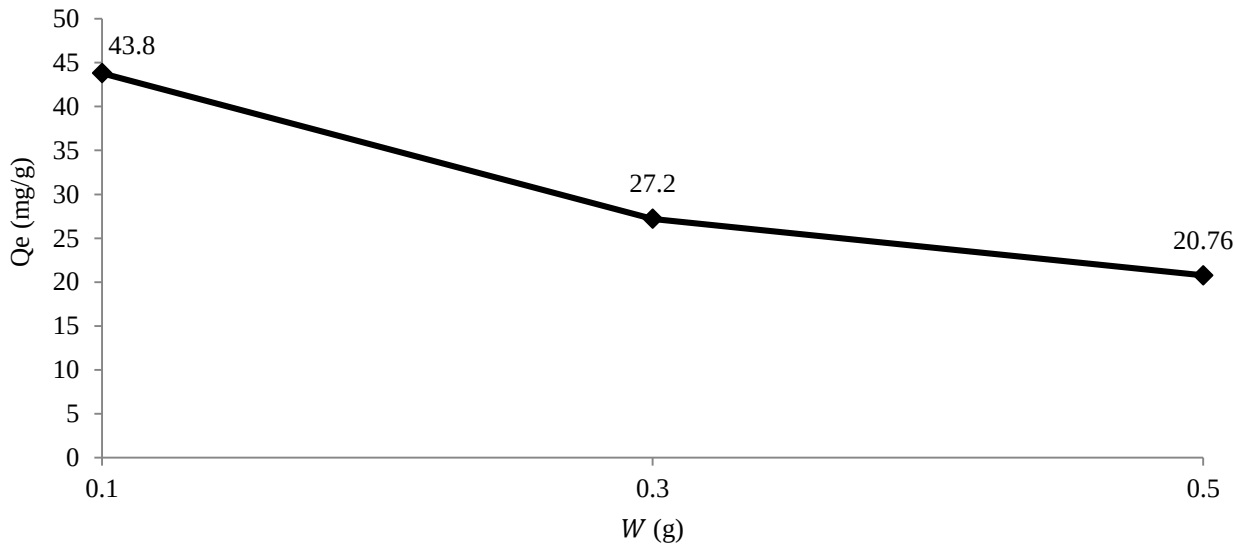

Figure 5. Amount of 2,4-DCP adsorbed, Q_e against mass of AC used

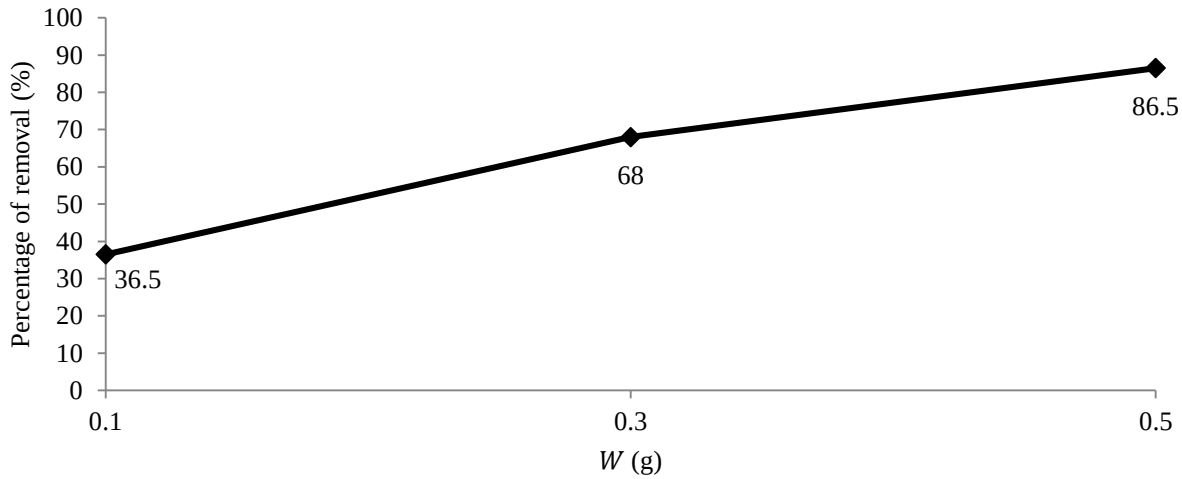

Figure 6. Percentage of removal against mass of AC used

Effect of solution pH

From Figure 7, the adsorption capacity decreases with an increase in the pH of the solution. In acidic pH (pH < pK_a of 2,4-DCP), the 2,4-DCP molecules exist in non-ionic form and the adsorption sites of AC are positively charged. This leads to the electrostatic attraction between the molecular form of 2,4-DCP and the adsorption sites. Therefore, an increase in the adsorption capacity of AC in low pH.

Alternatively, in basic pH (pH > pK_a of 2,4-DCP), the 2,4-DCP molecules dissociate into phenolate ions, while the surface functional groups of AC become neutral or negatively charged. This can cause electrostatic repulsion between phenolate ions and negatively charged adsorption sites, lowering adsorption capacity.

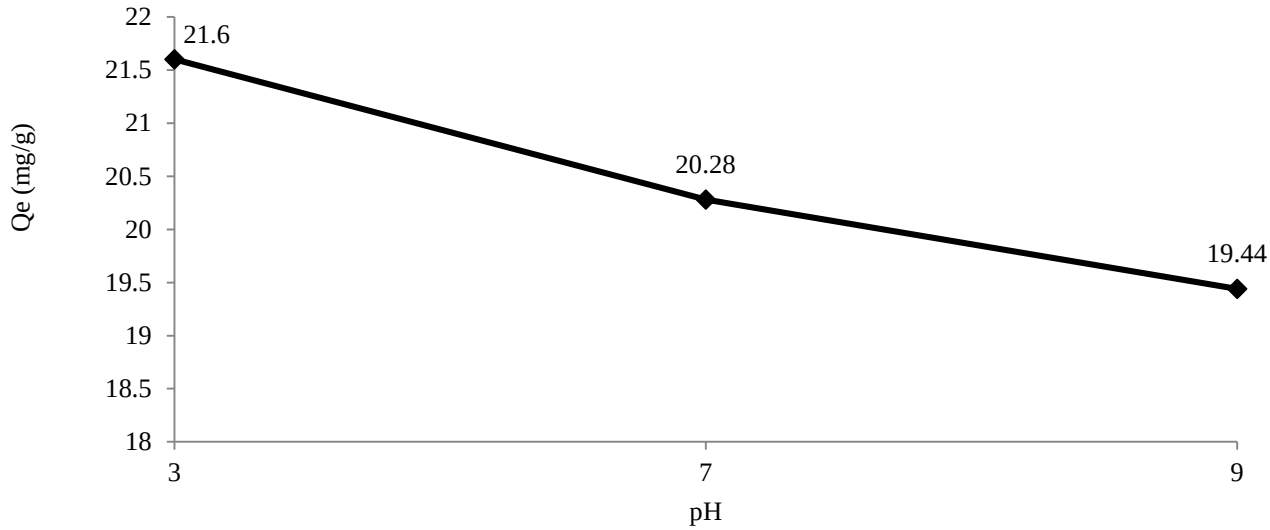

Figure 7. Amount of 2,4-DCP adsorbed, Q_e against pH.

Adsorption kinetics studies

The adsorption kinetics studies of 2,4-DCP onto AC4 were determined from the uptake analysis data. As shown in Figure 8, the amount of 2,4-DCP adsorbed by AC4 was increased rapidly for the first 20 min due to the many vacant adsorption sites present for the adsorption. However, after 20 min, the adsorption of 2,4-DCP became slower. This is because the adsorption sites are gradually saturated with the adsorbate molecules. At 180 min, the equilibrium was achieved in which the amount of 2,4-DCP adsorbed was 21.12 mg/g.

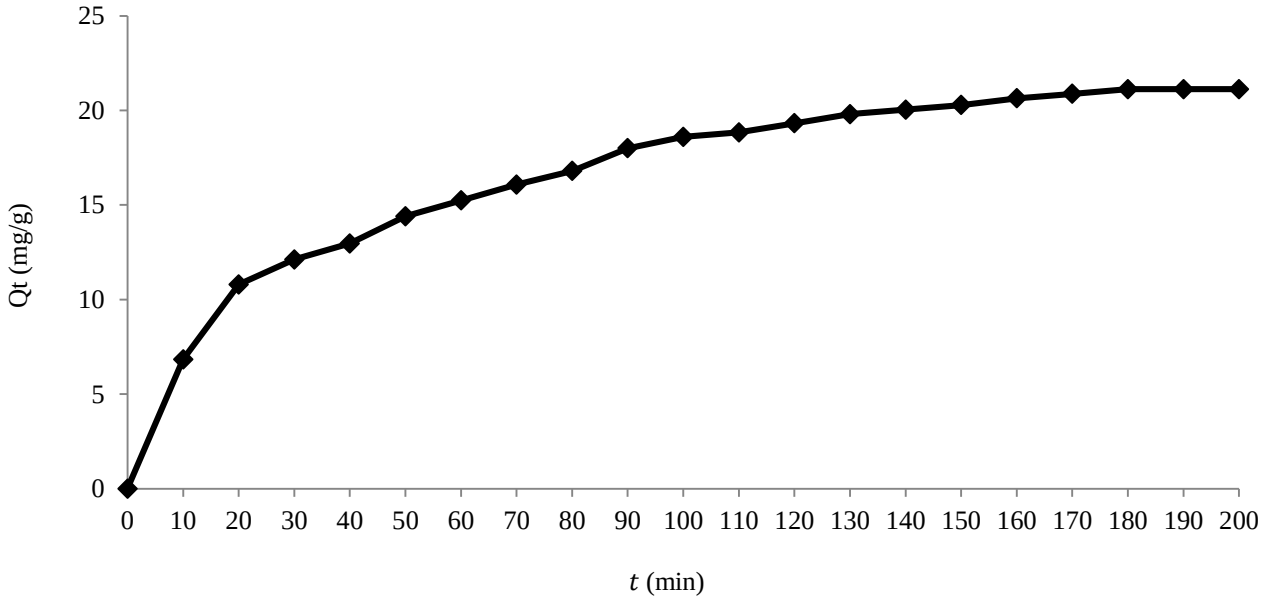

Figure 8. Amount of 2,4-DCP adsorbed at time t, Q_t against time

From the results demonstrated in Figure 9 (a,b), the adsorption kinetics of 2,4-DCP onto AC4 was best fitted into the pseudo-second order kinetic model with correlation coefficients, R^2 equals to 0.9971 which was more than the correlation coefficients of pseudo-first order kinetic model (R^2 = 0.9645). This verifies that chemisorption was the rate-controlling step which involves valence forces generated from the sharing and exchange of electrons between 2,4-DCP molecules and AC4 during the adsorption process. This result was in accordance with the previous research carried out on the adsorption of 2,4-DCP utilised AC prepared from palm pith [38].

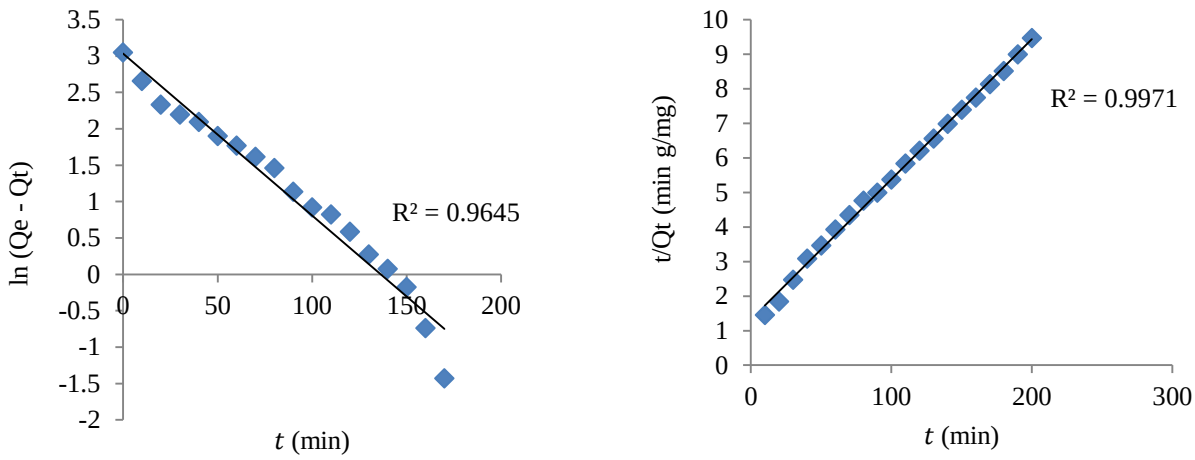

(a) (b)

Figure 9. Adsorption of 2,4-DCP onto AC4 (a) Pseudo-first order kinetic model (b) Pseudo-second order kinetic model

In order to understand the mechanism of 2,4-DCP adsorption by AC4, intraparticle diffusion kinetic model was applied. The plot shown in Figure 10 exhibited multi-linearity, indicating that the adsorption process can be divided into three stages (regions 1, 2, and 3). The sharper region 1 indicates the instantaneous adsorption or external surface adsorption. Region 2 with a smaller gradient signified the gradual adsorption stage where intraparticle diffusion was rate-limiting. As the intraparticle diffusion began to slow down, the final equilibrium stage was achieved (region 3). This was caused by the exceedingly low concentration of 2,4-DCP in the solution. On the other hand, intraparticle diffusion was not the rate-controlling step and there was some degree of boundary layer control as the linear lines did not pass through the origin [39]. From the intraparticle diffusion model equation, the thickness of boundary layer can be estimated through value a. The higher the value of a, the greater the boundary layer effect.

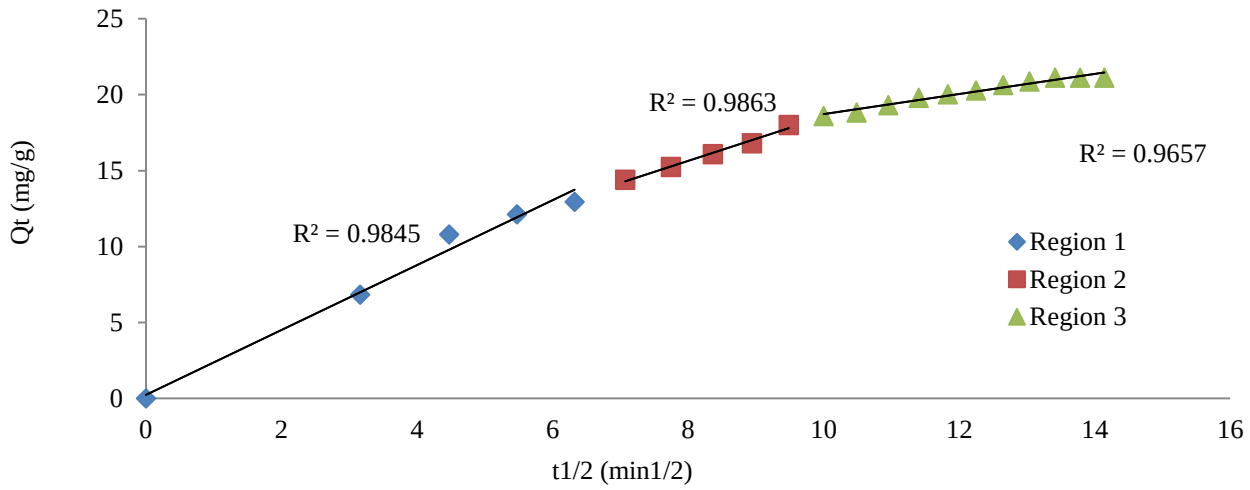

Figure 10. Intraparticle diffusion kinetic model for adsorption of 2,4-DCP onto AC4

As can be seen from Table 6, the value of k_{id} was decreased, whereas value a was increased from region 1 – 3. This showed the domination of the mass transfer process in the initial stage due to the high intraparticle diffusion rate and weak boundary layer effect. Subsequently, at a later stage, the intraparticle diffusion rate became gradually decreased and the boundary layer effect became gradually larger because of the possibility of steric hindrance or pore blockage caused by the adsorbed molecules on surface of AC4. Hence, the adsorption of 2,4-DCP onto AC4 was initially controlled by external mass transfer and then by intraparticle diffusion mass transfer.

Table 6. Kinetic parameters based on the intraparticle diffusion model

Region	k_{id} (mg/g min$^{1/2}$)	a (mg/g)	R^2
1	2.1359	0.2412	0.9845
2	1.4467	4.0633	0.9863
3	0.6636	12.079	0.9657

Adsorption isotherms studies

The data obtained from the initial concentration test was utilised in the adsorption isotherm studies. According to the fitting results shown in Figures 11,12 and 13, the Langmuir isotherm model was more suitable than the Freundlich and Tempkin isotherm models since the correlation coefficient of the Langmuir model (R^2 = 0.8110) was higher than Freundlich (R^2 = 0.7492) and Tempkin (R^2 = 0.5562). This indicated that AC4 had homogenous nature on its surface in which all molecules have equal enthalpies and activation energies during the adsorption process. This result also proved the monolayer adsorption of 2,4-DCP on the surface of AC4. Moreover, chemisorption was further verified through this outcome.

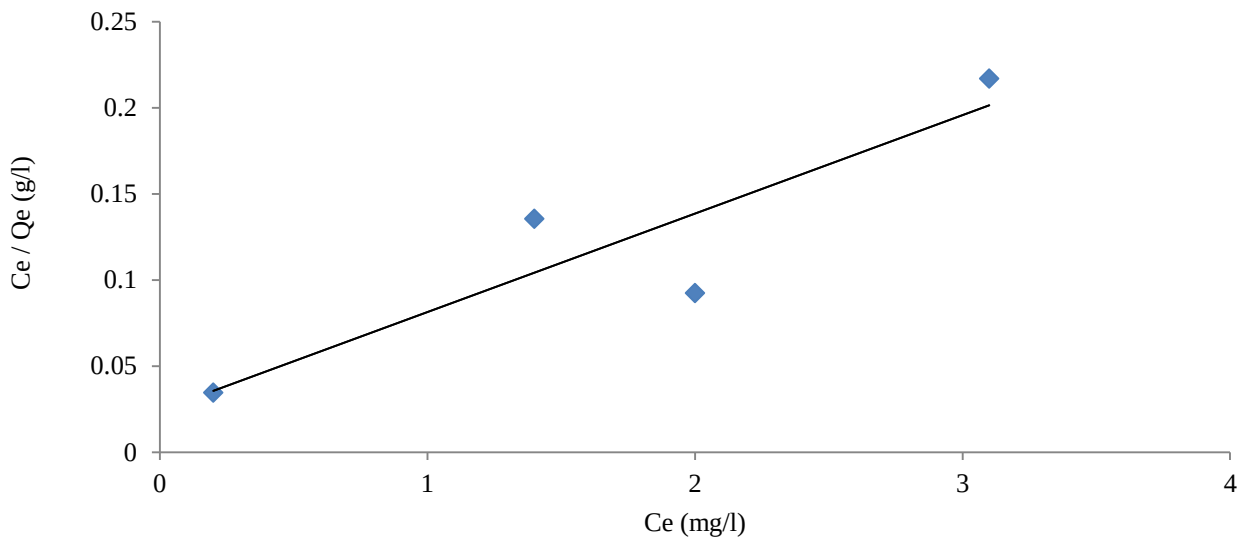

Figure. 11. Langmuir adsorption isotherm for adsorption of 2,4-DCP onto AC4.

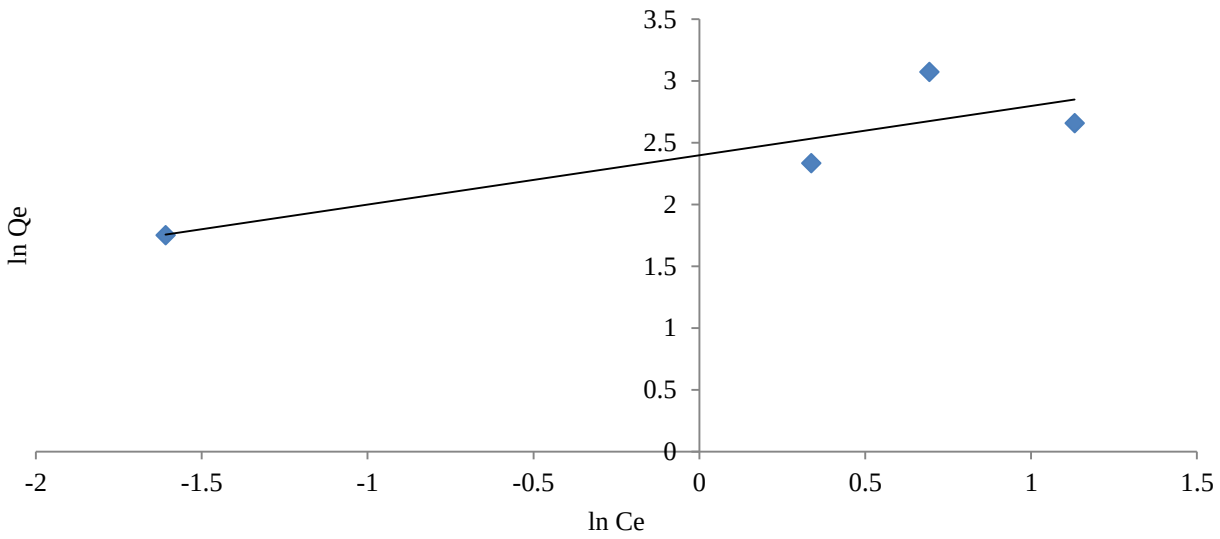

Figure. 12 Freundlich adsorption isotherm of 2,4-DCP onto AC4

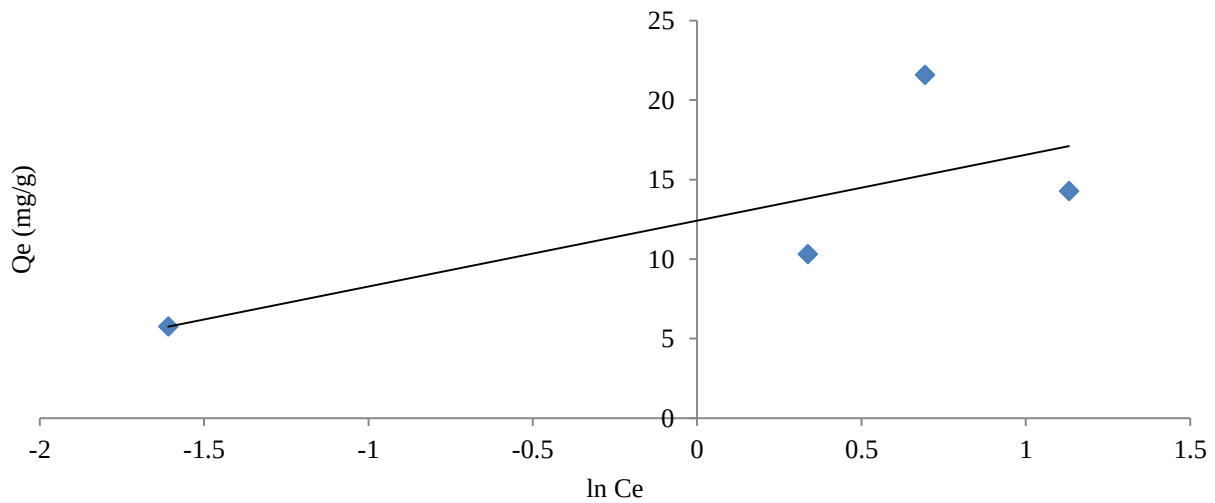

Figure 13. Tempkin adsorption isotherm of 2,4-DCP onto AC4

Comparison of the results from different studies

Table 7 shows the literature values of previous studies of AC using coffee grounds and waste for comparison.

Table 7. Comparison of previous studies of AC using coffee

Precursor	Activation method	Product quality	
Spent coffee grounds	Phosphoric acid activation had been employed as the adsorbent for ethylene and n-butane at room temperature.	BET surface area: 1110 m^2/g, Adsorption isotherms of ethylene and n-butane fitted well with Langmuir equation.	[40]
Coffee extract residue	Prepared ACs using both chemical and physical activation methods (H_3PO_4 at different concentrations: 30, 40 and 50%; heat-treatment temperatures were 500, 600, 700 and 800^oC.	Maximum surface area of >640 m^2/g with increased total pore and micropore volumes.	[25]
Coffee husks	Coffee husks were washed with distilled water and dried at 105^oC for 5 h in a convection oven. Afterwards they were treated with 2% formaldehyde solution	Biosorption data was best described by Langmuir model and pseudo second-order mechanism was confirmed for the biosorption kinetics. This study was demonstrated that coffee husks are suitable candidates for use as biosorbents in the removal of cationic dyes.	[41]
Coffee ground wastes	Acid black carbons from coffee waste were produced by simple pyrolysis at 673 K and then were sulfonated by sulphuric acid or fuming sulphuric acid.	The "apparent" surface area for all carbons obtained is very small (S_{BET} < 10 m^2/g). However, these acid carbons showed good catalytic activity in glycerol conversion, compared to the commercial resin,	[24]
Coffee residues	Coffee residues were contacted with H_3 PO_4 at an impregnation ratio 1:4. This material was dried in air at 100^oC for 3 h. The obtained sample was carbonized at 500^oC (5 C/min) under N_2 atmosphere (300 cm^3/ min) for 30 min.	BET surface area: 221.55 m^2/g ACs obtained from coffee residues are mesoporous. Their nitroimidazole adsorption capacity per unit of carbon surface area ranges between 0.91 $x10^3$ and 4.02 $x10^3$ $mmol/m^2$ and their sodium diatrizoate adsorption capacity ranges between 0.63$x10^3$ and 2.70 $x10^3$ $mmol/m^2$, which are higher capacities than previously reported in the literature.	[23]

Spent Coffee Grounds and Coffee Parchment	AC was prepared from spent coffee grounds and parchment through the co-calcination process and calcium carbonate ($CaCO_3$) was used to optimize the calcinations.	Spent coffee grounds and parchment showed yields after the calcination and washing treatments of around 9.0%. The adsorption of lactic acid was found to be optimal at pH 2. The maximum adsorption capacity of lactic acid was 32.33 and 14.73 mg/g for the parchment and spent coffee grounds ACs, respectively.	[42]
Coffee waste	ACs were prepared from coffee waste via two-stage self-generated atmosphere method after impregnation by $ZnCl_2$.	BET surface area: 951.10 m^2 /g, In this study, the removal of 2,4-DCP in aqueous medium by AC samples was effectively demonstrated and highest adsorption capacity found to be 21.72 mg/g . Kinetics of 2,4-DCP adsorption was best described by pseudo-second order kinetic model.	This study

CONCLUSIONS

Based on the data obtained, it can be concluded that coffee waste can be effectively utilised to prepare AC via $ZnCl_2$ activation in a two-stage self-generated atmosphere method. It was found that the IR of $ZnCl_2$ can affect the characteristics of the AC samples generated. High yield of AC samples was produced using this method in which the yield percentage was decreased from 41.16% to 37.12% for the increasing IR. As for moisture and ash contents, the percentage values were ranged from 4.18% to 6.16% and 9.73% to 10.34% respectively. The ash content increased with the increasing IR. Meanwhile, the AC samples were slightly acidic with pH values varying between 6.06 and 6.56. Besides that, the morphology of AC samples was greatly affected by IR as proved by the SEM micrographs. Various functional groups were present on the surface of AC samples as demonstrated by the FT-IR spectra. However, the surface functional groups of AC samples were generally not influenced by the IR. On the other hand, the removal of 2,4-DCP in an aqueous medium by AC samples was also effectively demonstrated. AC4 yielded the highest 2,4-DCP adsorption capacity which is 21.72 mg/g compared to other samples. Furthermore, the adsorption capacity of AC4 was found to increase with the increased initial concentration of 2,4-DCP and decreasing adsorbent dosage. Nevertheless, an increased in adsorbent dosage resulted in the increment of the percentage of 2,4-DCP removal. The adsorption of 2,4-DCP was found to be more favourable in an acidic solution. The kinetics of 2,4-DCP adsorption by AC4 was best described by the pseudo-second order kinetic model, while the adsorption equilibrium data was well fitted to the Langmuir isotherm model, indicating that chemisorption was a rate limiting step.

ACKNOWLEDGEMENTS

This study was supported by the Research Management Centre of Universiti Malaya in collaboration with the Research Management Centre of Universiti Malaysia Sabah (UMS) (Grant no. GL0111 or UM Project code: CG071-2013). These contributions are gratefully acknowledged. The authors also pay their sincere gratitude to UMS for providing necessary research facilities to accomplish this study.

REFERENCES

Afsharnia, M., Saeidi, M., Zarei, A., Narooie, M. R. and Biglari, H. (2016) Phenol removal from aqueous environment by adsorption onto pomegranate peel carbon, *Electron. Physician,* **8(11),** 3248-3256.

Malakootian, M., Mansoorian, H. J., Alizadeh, M. and Baghbanian, A. (2017) Phenol removal from aqueous solution by adsorption process: Study of the nanoparticles performance prepared from aloe vera and mesquite (Prosopis) leaves, *Sci. Iran.,* **24(6),** 3041-3052.

Palanisamia H, Mohamad R. M. A., Muhammad A. A. Z, Zakariaa Z. A., Alama M. Z. H. Z. and Yunusa M. A. C. (2021) Coffee residue-based activated carbons for phenol removal , *Water Pract. Technol* ., **16(3),** 793-805.

Anku, W. W., Mamo, M. A. and Govender, P. P. (2017) Phenolic compounds in water: sources, reactivity, toxicity and treatment methods. In: Phenolic Compounds – Natural Sources, Importance and Applications (Soto-Hernandez, M., Palma-Tenango, M. & del Rosario Garcia-Mateos, M., eds). IntechOpen, London.

Yousef, R., Qiblawey, H. and El-Naas, M. H. (2020) Adsorption as a process for produced water treatment: a review, *Processes,* **8(1657),** 1-22.

Girish. C. R. and George, G. M. (2017) Phenol removal from wastewater using arecanut husk (areca catechu) as adsorbent, *Int. J. Mech. Eng. Technol,* **8(12),** 1-9.

Tabassi, D., Soumaya, H., Islem, L. and Bechir, H. (2017) Response surface methodology for optimisation of phenol adsorption by activated carbon: Isotherm and kinetic study, *Indian J. Chem. Technol.,* **24(3),** 239-255.

Yan, K. Z., Ahmad-Zaini, M. A., Arsad, A. and Nasri, N. S. (2019) Rubber seed shell based activated carbon by physical activation for phenol removal, *Chem. Eng. Trans.,* **72,** 151–156.

Mohammed, N. A. S., Abu-Zurayk, R. A., Hamadneh, I. and Al-Dujaili, A. H. (2018) Phenol adsorption on biochar prepared from the pine fruit shells: equilibrium, kinetic and thermodynamics studies. J.Environ.Manage., **226,** 377–385.

Tzvetkova, P. G., Nickolov, R. N., Tzvetkova, C. T., Bozhkov, O. D. and Voykova, D. K. (2016) Diatomite/carbon adsorbent for phenol removal, *J. Chem. Technol. Metall,* **51(2),** 202-209.

Huu, S. T., Khu, L. V, Thu, T. L. T. and Thanh, H. H. (2020). Kinetic studies on the adsorption of phenol from aqueous solution by coffee husk activated carbon, *Mediterr. J. Chem.,* **10(7),** 676-686.

Anisuzzaman, S. M., Bono, A., Krishnaiah, D. and Tan, Y. Z. (2016) A study on dynamic simulation of phenol adsorption in activated carbon packed bed column, *J. King Saud Univ. Eng. Sci.,* 28(1), 47-55.

Daffalla, S. B., Mukhtar, H. and Shaharun M. S. (2020) Preparation and characterization of rice husk adsorbents for phenol removal from aqueous systems, *PLoS One,* **15(12):** e0243540.

Crini, G. and Lichtfouse, E. (2018). Advantages and disadvantages of techniques used for wastewater treatment, *Environ. Chem. Lett.,* **17,** 145-155.

Sales, F. R. P., Serra, R. B. G., Figueirêdo, G. J. A. D., Hora, P. H. A. D. and Sousa, A. C. D. (2019) Wastewater treatment using adsorption process in column for agricultural purposes, *Rev. Ambient. Água.,* **14(1),** 1-9.

Agrawal, V. R., Vairagade, V. S. and Kedar, A. P. (2017) Activated carbon as adsorbent in advance treatment of wastewater, *IOSR J. Mech. Civ. Eng.,* **14(4),** 36-40.

Adeleke, O. A., Latiff, A. A. A., Saphira, M. R., Daud, Z., Ismail, N., Ahsan, A., Aziz, N. Adila A., Ndah, M., Kumar, V., Adel Al-Gheethi, Rosli, M. A. and Hijab, M. (2019) Locally derived activated carbon from domestic, agricultural and industrial wastes for the treatment of palm oil mill effluent, *Nanotechnology in Water and Wastewater Treatment,* **2,** 35-62

Gawande, P. R. and Kaware, J. (2017) Characterization and activation of coconut shell activated carbon, *Int. J. Eng. Sci. Invention,* 6(11) 43-49.

Saleem. J., Shahid, U., Hijab, M., Mackey, H. and McKay, G. (2019) Production and applications of activated carbons as adsorbents from olive stones, *Biomass Convers. Biorefin.,* 9, 775-802.

Ukanwa, K. S., Patchigolla, K. Sakrabani, R. and Anthony, E. (2020) Preparation and characterisation of activated carbon from palm mixed waste treated with trona ore, *Molecules.* **25(21): 5028**, 1-18.

Saeed, A. A. H., Harun, N. Y., Sufian, S., Bilad, M. R., Nufida, B. A., Ismail, N. M., Zakaria, Z. Y., Jagaba, A. H., Ghaleb, A. A. S. and Al-Dhawi, B. N. S. (2021) Modeling and optimization of biochar based adsorbent derived from kenaf using response surface methodology on adsorption of Cd2+," *Water,* **13(7),** 1-18.

Ekpete. O. A., Marcus, A. C. and Osi, V. (2017) Preparation and characterization of activated carbon obtained from plantain (*Musa paradisiaca*) fruit stem, *J. Chem.,* **2017 (8635615),** 1-6.

Flores-Cano, J. V., Sanchez-Polo, M., Messoud, J., Velo-Gala, I., Ocampo-Perez, R. and Rivera-Utrilla, J. (2016) Overall adsorption rate of metronidazole, dimetridazole and diatrizoate on activated carbons prepared from coffee residues and almond shells, *J. Environ. Manage.,* **169,** 116-125.

Gonçalves, M., Soler, F. C., Isodaa, N., Carvalhoa, W. A., Mandelli, D. and Sepúlvedac, J. (2016) Glycerol conversion into value-added products in presence of a green recyclable catalyst: Acid black carbon obtained from coffee ground wastes, *J. Taiwan Inst. Chem. Eng.,* **60,** 294-301.

Tehrani, N. F., Aznar, J. S. and Kiros, T. (2015) Coffee extract residue for production of ethanol and activated carbons, *J. Clean. Prod.,* **91,** 64-70.

Ahmad, M. A. and Rahman, N. K. (2011) Equilibrium, kinetics and thermodynamic of Remazol Brilliant Orange 3R dye adsorption on coffee husk-based activated carbon. *Chem. Eng. J.l,* **170(1),** 154-161.

Lamine, S. M., Ridha, C., Mahfoud, H.-M., Chenine, Mouad, Lotfi, B. and Al-Dujaili A. H. (2014) Chemical activation of an activated carbon prepared from coffee residue, *Energy Procedia,* **50**, 393-400.

Boonamnuayvitaya, V., Sae-ung, S. and Tanthapanichakoon, W. (2005) Preparation of activated carbons from coffee residue for the adsorption of formaldehyde, *Sep. Purif. Technol.,* **42(2),** 159-168.

Namanea, A., Mekarzia, A., Benrachedi, K., Belhaneche-Bensemra, N. and Hellal, A. (2005) Determination of the adsorption capacity of activated carbon made from coffee grounds by chemical activation with $ZnCl_2$ and H_3PO_4, *J. Hazard. Mater.,* **119(1-3),** 189-194.

Wang, X., Liang, X., Wang, Y., Wang, X., Liu, M., Yin, D., Xia S., Zhao J. and Zhang Y. 2011. Adsorption of Copper (II) onto activated carbons from sewage sludge by microwave-induced phosphoric acid and zinc chloride activation, *Desalination,* **278**(1-3), 231-237.

Uysal, T., Duman, G., Onal, Y., Yasa, I. and Yanik, J. (2014) Production of activated carbon and fungicidal oil from peach stone by two-stage process, *J. Anal. Appl. Pyrolysis,* **108**, 47-55.

Metin A, Gürses, A. and Karaca, S. 2014. Preparation and characterization of activated carbon from plant wastes with chemical activation, *Microporous Mesoporous Mater.,* **198**, 45-49.

Ozdemir, I., Şahin, M., Orhan, R. and Erdem, M. (2014) Preparation and characterization of activated carbon from grape stalk by zinc chloride activation, *Fuel Process. Technol.,* **125**, 200-206.

Zhong, Z., Yang, Q., Li, X., Luo, K., Liu, Y. and Zeng, G. (2012) Preparation of peanut hull based activated carbon by microwave-induced phosphoric acid activation and its application in Remazol Brilliant Blue R adsorption. *Ind. Crop. Prod.*, **37(1),** 178-185.

Özdemir, M., Bolgaz, T., Saka, C. and Sahin, Ö. (2011) Preparation and characterization of activated carbon from cotton stalks in a two-stage process, *J. Anal. Appl. Pyrolysis*, **92(1),** 171-175.

Anisuzzaman, S. M. Joseph C. G., Krishnaiah D., Bono A., Suali E., Abang S. and Fai L. M. (2016) Removal of chlorinated phenol from aqueous media by guava seed (*Psidium guajava*) tailored activated carbon, *Water Res. Ind.*, **16**, 29-36.

Krishnaiah, D., Joseph, C. G., Anisuzzaman, S. M., Daud, W. M. A. W., Sundang M., and Leow, Y. C. (2017) Removal of chlorinated phenol from aqueous solution utilizing activated carbon derived from papaya (*Carica Papaya*) seeds, *Korean J. Chem. Eng.*, **34(5)**, 1377-1384.

Sathishkumar, M., Binupriya, A. R., Kavitha, D. and Yun, S. E. (2007) Kinetic and isothermal studies on liquid-phase adsorption of 2,4-dichlorophenol by palm pith carbon. *Bioresour. Technol.*, **98(4),** 866-873.

Yakout, S. M. and Elsherif, E. 2010. Batch kinetics, isotherm and thermodynamic studies of adsorption of strontium from aqueous solutions onto low cost rice-straw based carbons. *Carbon - Sci. Tech.*, **1**, 144-153.

Ma, X. and Ouyang, F. (2013) Adsorption properties of biomass-based activated carbon prepared with spent coffee grounds and pomelo skin by phosphoric acid activation, *Appl. Surf. Sci.*, **268,** 566-570.

Oliveira, L. S., Franca, A. S., Alves, T. M. and Rocha, S. D. F. (2008) Evaluation of untreated coffee husks as potential biosorbents for treatment of dye contaminated waters, *J. Hazerd. Mater.*, 155(3), 507-512.

Campos G. A. F., Perez J. P. H., Block I., Sagu S. T., Celis P. S., Taubert A. and Rawel H. M. (2021) Preparation of activated carbons from spent coffee grounds and coffee parchment and assessment of their adsorbent efficiency, *Processes*, 9(1396), 1-18.